

## High frequency resonant experiments in $\text{Fe}_8$ molecular clusters.

E. del Barco, J.M. Hernandez, and J. Tejada.

*Dept. de Física Fonamental, Universitat de Barcelona, Diagonal 647,  
08028 Barcelona, Spain.*

N. Biskup, R. Achey, I. Rutel, N. Dalal, and J. Brooks

*NHMFLL, CM/T group 1800 E.P.Dirac dr. Tallahassee, FLORIDA 32310*

Precise resonant experiments on  $\text{Fe}_8$  magnetic clusters have been conducted down to 1.2 K at various transverse magnetic fields, using a cylindrical resonator cavity with 40 different frequencies between 37 GHz and 110 GHz. All the observed resonances for both single crystal and oriented powder, have been fitted by the eigenstates of the hamiltonian  $\mathcal{H} = -DS_z^2 + ES_x^2 - g\mu_B \mathbf{H} \cdot \mathbf{S}$ . We have identified the resonances corresponding to the coherent quantum oscillations for different orientations of spin  $S = 10$ .

PACS number(s): 75.45+j

At low temperature magnetic molecules with spin  $S = 10$ ,  $\text{Mn}_{12}$  and  $\text{Fe}_8$ , are equivalent to a single domain particle with a constant magnetic moment,  $m = 20\mu_B$ . The orientation of this magnetic moment freezes, however, along one of two easy directions when temperature becomes small compared to the energy barrier height due to magnetic anisotropy. The discovery of resonant spin tunneling was first achieved by performing both hysteresis measurements and relaxation experiments on  $\text{Mn}_{12}$ -acetate below that blocking temperature [1–4]. More recently new experimental proofs of this effect have been obtained by using different experimental techniques [5–8]. Comprehensive theories for the tunneling rate in the presence of phonons were developed which explain quantitatively the experimental results [9–11]. Very recently two new experiments have brought more excitement to this field. Wernsdorfer et al. [12] have detected the suppression of the spin tunneling rate in  $\text{Fe}_8$  due to the non-Kramers topological quenching of tunneling noticed by Garg [13]. Del Barco et al. [14] have detected the coherent quantum oscillations of the spin 10 in  $\text{Fe}_8$  by performing resonance experiments at 680 MHz. In this paper we report the results of high frequency experiments on  $\text{Fe}_8$ , between 37 GHz and 110 GHz, in the Kelvin regime. This experiment follows the pioneering idea of Awschalom et al. [15] on the search of quantum coherence of the spin in nanomagnets by performing resonant experiments.

The material studied is composed by  $\text{Fe}_8$  single crystals synthesized according to ref. [16]. The magnetic susceptibility data support the non existence of paramagnetic impurities and the measured crystal cell parameters are in full agreement with those previously published [16]. The experiments were carried out on a single crystal of 2 mm length and on a oriented powder sample composed of small crystallites of 1  $\mu\text{m}$  average size. The orientation of the the powder was done by solidifying an

epoxy with the  $\text{Fe}_8$  microcrystallites buried inside and applying during 12 h, the solidifying time of the epoxy, a magnetic field of 5.5 T. The nominal composition,  $[(C_6H_{15}N_3)_6Fe_8(\mu_3-O)_2(\mu_2-OH)_{12}(Br_7(H_2O))Br_8H_2O]$ , was checked by chemical and infrared analysis. The single crystal was placed on the cavity of the resonator with its hard plane ( $xy$  plane) mostly parallel to the applied field. It was nevertheless a small misalignment angle,  $\theta$ , between the direction of the applied magnetic field and the hard plane. In fact this angle is the only fitting parameter we used in our fitting procedure.

The occurrence of resonant spin tunneling in  $\text{Fe}_8$  was first detected by Sangregorio et al. [17]. The spin hamiltonian has been deduced from EPR experiments [18]. The ac susceptibility data published by Zhang et al. [19] on an oriented powder sample of  $\text{Fe}_8$  are in agreement with those above mentioned. Our materials were characterized by performing dc and ac magnetic measurements on both single crystal and oriented powder. Both samples show periodic steps in the magnetic data, separated by a period of 0.24 T. We have also performed magnetic susceptibility measurements at different fields down to 100 mK. The zero field cooled (ZFC) and field cooled (FC) curves merge at 0.8K. A Curie-Weiss behaviour is observed between this temperature and few K which corresponds to the only population of the level  $S = 10$ . The Curie temperature deduced from this low temperature susceptibility data is 0.5 K which is the measure of the interaction between the molecules. At higher temperature strong deviations from the Curie-Weiss is observed due to the population of levels with  $S < 10$  as it was first experimentally demonstrated by Delfs et al. [20].

To the first approximation, the Hamiltonian of  $\text{Fe}_8$  is [17,18]:

$$\mathcal{H} = -DS_z^2 + ES_x^2 - g\mu_B \mathbf{H} \cdot \mathbf{S} + C(S_+^4 + S_-^4) \quad (1)$$

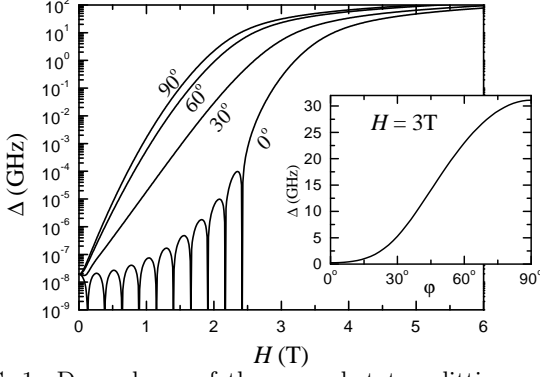


FIG. 1. Dependence of the ground-state splitting on the transverse field in Fe<sub>8</sub> for different angles  $\varphi$ . The inset shows the angular dependence of the splitting at a fixed value of the field  $H = 3$  T.

where  $z$  and  $x$  denote the easy and hard axes respectively. The values of  $D = 0.229$  K,  $E = 0.093$  and  $C = 2.9 \cdot 10^{-5}$  K are known from EPR, neutron spectroscopy and magnetic relaxation experiments [17,18,21,12].  $H$  is the applied magnetic field. The component of the applied magnetic field parallel to the easy axis direction, called longitudinal component,  $H_{\parallel} = H \sin \theta$ , changes the barrier height between the two classical spin orientations, while the component of the field on the hard plane, transverse component,  $H_{\perp} = H \cos \theta$ , affects the overlapping of the respective wave functions, which determines the quantum splitting of the degenerate spin states. The quantum splitting,  $\Delta$ , and consequently the rate of resonant tunneling between the spin levels depend on both the magnitude of the transverse component  $H_{\perp}$  and its angle  $\varphi$  with the hard axis. The dependence of the quantum splitting of the ground state,  $S_z = 10$ , on the applied magnetic field,  $\Delta(H_{\perp})$  is shown in figure 1. The angular dependence of  $\Delta(\varphi)$  at a fixed value of the transverse component of the field,  $H_{\perp} = 3$  T, obtained by numerical diagonalisation of the Hamiltonian (1) is plotted in the inset of Figure 1. Because of the shape of the function  $\Delta(\varphi)$ , for a sample with hard axis oriented at random, that is with not preference for any angle  $\varphi$ , there are two values of  $\Delta$  for which the density of states has a peak. These are the values of the splitting corresponding to  $\varphi = 0$  and  $\varphi = \frac{\pi}{2}$ .

The evolution of the spin levels in the two wells as a function of the intensity of the transverse component of the field, as deduced from the diagonalisation of the spin hamiltonian, is shown in Figure 2. The resultant spin levels on the left side of line 1 correspond to the quantum splittings of the different  $S_z$  levels due to tunneling. In the case of the lowest  $|S_z| = 10$  level, the tunneling gives rise to the true ground state and the first excited state which are separated by the energy  $\Delta_{10}$ . The probability of the spin of each Fe<sub>8</sub> molecule to have a certain orientation  $\mathbf{S}$ , at a moment of time  $t$  is given by  $P(t) = \cos(\Gamma t)$ . Consequently our system of Fe<sub>8</sub> molecules placed in an  $ac$  field of frequency  $\omega$  will show a resonance in the power

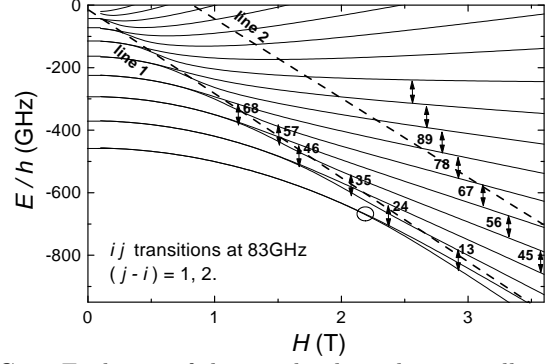


FIG. 2. Evolution of the spin levels in the two wells on the intensity of the transverse field for  $\varphi = \frac{\pi}{2}$ . Lines 1 and 2 limit the transition zone between the quantum splittings of the  $S_z$  levels (low frequency) and the strongly mixed  $S_z$  states (high frequency). Open circle at 2.25 T in the lowest level indicates the absorption peak corresponding to a frequency of 680 MHz extracted from ref. 14

spectrum if  $\omega = \Delta_{10}/\hbar = \Gamma$ . To observe this resonance and those associated with different  $S_z$  levels, the dissipation should be small compared to the quantum splitting. Dissipating destroys the coherence of spin quantum oscillations after a certain decoherence time. This is the reason why it is necessary to carry out experiments at high fields (large splittings) and, consequently, high frequencies. The transverse component of the magnetic field must be, nevertheless, smaller than the anisotropy field,  $H_a$ , to have degenerate spin levels. These are the levels on the left on line 1 in Figure 2. For  $H_{\perp}$  values greater than the anisotropy field the labeling of the spin levels is more complicate as they result from strongly mixing of the  $S_z$  states. That is, in this high-field regime, on the right of line 2, the appropriate eigenstates are  $S_x$  and  $S_y$  depending on the direction of the applied magnetic field. Between these two lines, there is an intermediate region in which for a given  $H_{\perp}$  value there are both types of levels.

In the absence of dissipation, the contribution of each Fe<sub>8</sub> crystallite to the imaginary part of the susceptibility is proportional to  $\delta(\omega - \frac{\Delta[\varphi, H_{\perp}]}{\hbar})$ . However, the total imaginary part of the susceptibility is,

$$\chi'' \propto \int_0^\pi g(\varphi) \delta(\omega - \frac{\Delta[\varphi, H_{\perp}]}{\hbar}) d\varphi, \quad (2)$$

where  $g(\varphi)$  is the distribution of crystallites on  $\varphi$ . For a single crystal, having all its molecules with  $x$  axis exactly at the same angle, the amplitude  $A$  of the absorption of electromagnetic radiation must have only one peak corresponding to  $\Delta[\varphi, H_{\perp}] = \omega$ . For an oriented powder where there is a random orientation of the  $x$  axis of each crystallite, Eq. 2 can be rewritten as

$$\chi'' \propto \int_0^\infty \delta(\omega - \frac{\Delta[\varphi, H_{\perp}]}{\hbar}) \left( \frac{d\Delta}{d\varphi} \right)^{-1} d\Delta = \left( \frac{d\Delta}{d\varphi} \right)^{-1} \Big|_{\Delta=\hbar\omega}. \quad (3)$$

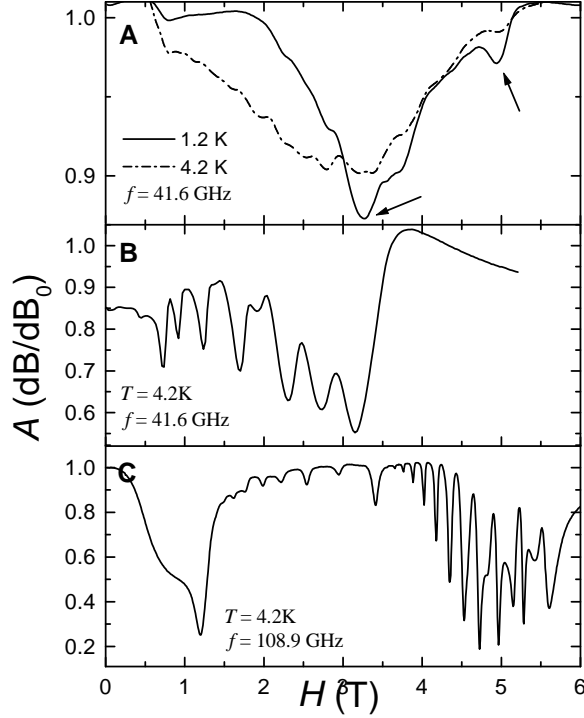


FIG. 3. Oriented powder (A) and single crystal absorption vs. magnetic field spectra (C,D) at various frequencies and temperatures. Arrows in fig. A point to the two peaks corresponding to  $\varphi = \frac{\pi}{2}$  ( $H = 3.2$  T) and  $\varphi = 0$  ( $H = 4.9$  T) orientations of the field on the hard plane.

Therefore, there are two field values, solutions of the equations  $\Delta[0, H_{\perp 1}] = \omega$  and  $\Delta[\frac{\pi}{2}, H_{\perp 2}] = \omega$ , at which the amplitude of the absorption is maximal.

The high frequency resonance experiments have been carried out using the AB millimeter wave vector network analyzer (MVNA) [22]. The base frequency obtained from this source (range 8 - 18 GHz) is multiplied by Q, V and W Schottky's diodes to obtain frequency range used in our experiment (37 - 109 GHz). The sample, a single  $\text{Fe}_8$  crystal or the oriented powder, is placed on the bottom of the cylindrical resonant cavity, halfway between its axis and perimeter. The applied dc magnetic field is parallel to the cavity axis and approximately perpendicular to the easy (c) axis of the crystal. The experiment frequencies are  $\text{TE}_{0np}$  ( $n, p = 1, 2, 3, \dots$ ) which are the resonant frequencies for the cavity used. Resonance Q-factor varies from 20000 at  $\text{TE}_{011}$  mode (41.6 GHz) to few thousand at higher frequencies. Due to high resonance sensitivity, we may detect all absorption peaks suggested theoretically by the diagonalization of the Hamiltonian of Equation 1.

The data for the  $\text{Fe}_8$  single crystal were obtained at  $T = 4.2$  K while  $T$  was varied between 1.2 K to 10 K for the oriented powder sample. Figure 3 shows the absorption curves for the two samples; figure 3A shows the spectra for the powder sample at two different temperatures and  $f = 41$  GHz. The most pronounced peaks shift to lower fields as the temperature is increased. Figures

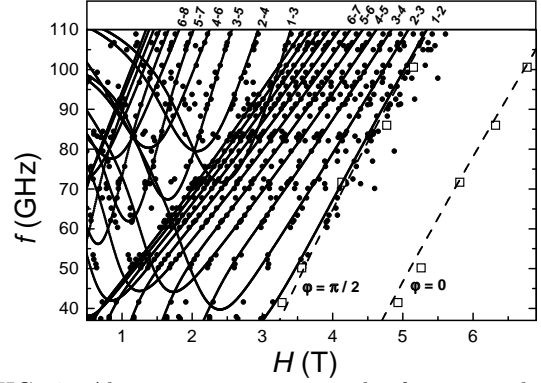


FIG. 4. Absorption resonant peaks for oriented powder (open squares) and single crystal (solid circles). The lines represent the theoretical calculations from the diagonalization of the Hamiltonian (1) for  $\varphi = \frac{\pi}{2}$  in the case of single crystal (solid lines), and for  $\varphi = 0$  and  $\varphi = \frac{\pi}{2}$  for the oriented powder (dashed lines).

3B and 3C show the resonance spectrum for the single crystal at two different frequencies; The resonant fields shift to higher fields when increasing the frequency. The resonance spectrum for the single crystal at  $T = 4.2$  K and  $f = 41$  GHz, has only peaks for field values lower than 3.2 T, while the spectrum for the oriented powder at the same temperature and frequency shows peaks until 5.2 T.

In Figure 4 we collect the values for the resonant peaks for the single crystal when using 40 different frequencies (solid circles). We also show in this figure (open squares) the values of the resonances for five different frequencies and  $T = 1.2$  K for the oriented powder. In this case we have selected the two most pronounced peaks for each frequency.

The position of the maximum of the resonant peaks (all of them have been collected in Figure 4) has been fitted by using the level structure (figure 2) resulted from the diagonalisation of the Hamiltonian (1). In this fitting procedure we have taken into account a small deviation, angle  $\theta$ , of the applied magnetic field from the hard plane of the crystal. The angle  $\theta$  of misalignment was the only fitting parameter used in our calculations. The resonant peaks for the oriented powder have been fitted without considering such misalignment because in this case there are always molecules, a fraction of  $10^{-6}$  of the total number of molecules in the sample, with their easy axis perpendicular to the applied magnetic field. For both samples, we have considered the occurrence of all possible transitions between spin levels  $i$  and  $j$  such that  $j - i = 1$  and  $j - i = 2$ . Each  $S_z$  level splits in two levels which, for example, at low fields are the symmetric and antisymmetric combinations of  $S_z$ . The levels appearing from  $S_z = 10$  are labeled 1 and 2, those from  $S_z = 9$  are labeled 3 and 4 and so on. The results of our fitting procedure are shown in Figure 4, solid lines correspond to the single crystal and the dashed lines correspond to the powder.

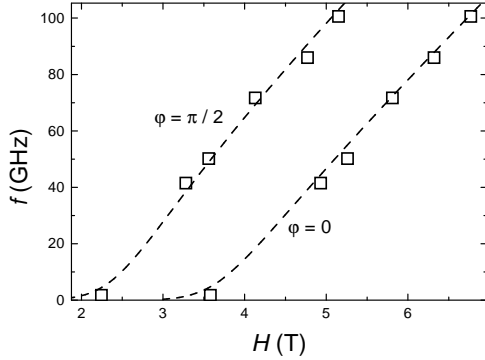


FIG. 5. Evolution of the quantum splitting of the ground state as a function of the intensity of the transverse field. Open squares represent the experimental points for the two orientations  $\varphi = 0$  and  $\varphi = \frac{\pi}{2}$  (powder sample) and the dashed line is the theoretical fitting. The low frequency points correspond to the frequency  $f = 680$  MHz and were extracted from Ref. 14

Let us discuss first the data for the powder sample. In Figure 4 we show the fitting (dashed lines) for the resonant peaks at four different frequencies (experimental values are open squares). First, we observe the existence of two resonant field values for each frequency which correspond to the energy absorption for the cases when the magnetic field is parallel and perpendicular to the hard axis, see Figure 1. The two peaks at 40 GHz observed at  $H_1 = 3.2$  T and  $H_2 = 4.9$  T correspond to the quantum splitting of  $S_z = \pm 10$  states for the two field orientations above mentioned. Although we do not know the decoherence characteristic time, the large values of the used frequency are likely to be in the coherence range. Then the two resonant peaks correspond to the quantum coherent oscillations of the spin between the levels  $S_z = +10$  and  $S_z = -10$  in all molecules. At higher frequencies, the resonant fields are larger than the barrier height and the  $ij$  transitions are the transitions between mixed levels, that is, the levels on the right of line 2 in Figure 2.

We have also been able to fit all the resonances observed in the single crystal for 40 different frequencies. In this case, we also have the angle  $\theta$  of misalignment, which is also the only fitting parameter. The angle  $\varphi$  takes only one value,  $\varphi = \frac{\pi}{2}$ , which is the angle between the applied magnetic field and the  $x$  axis of all molecules ( $x$  axis of the single crystal). The data are shown in Figure 4 in which the black points are the experimental data and the solid lines are the result of our fitting procedure after the diagonalisation of the spin Hamiltonian for the field values and frequencies used. As it is shown in that figure, all the transitions correspond to either  $ij$  transitions with  $j - i = 1$  or  $j - i = 2$ . It is important to notice that the transitions  $ij = 12, 34, 56, 78$ , etc., observed for field values lower than the barrier height of each level, correspond to the quantum splitting of different  $S_z$  levels. We are also observing high frequency transitions at

low fields which correspond to transitions between different, non-consecutive ( $j - i = 2$ ),  $S_z$  levels. Though the field dependence of such transitions is complicate, our fitting procedure was able to reproduce all the observed transitions.

In a previous paper [14] we discussed the results obtained at much lower frequency, 680 MHz. In Figure 5 we show, in a logarithmic plot, the resonant field values assigned to the quantum splitting,  $\Delta_{10}$ , of the  $S_z = \pm 10$  states for the two set of experiments. In the same Figure 5 we also show the result for the fitting of these data by the theoretical dependence of  $\Delta_{10}$  on the transverse field. The agreement between theory and experiment is remarkable, and confirms our interpretation. Moreover, the resonant field values for the peaks observed at 680 MHz are such that it is possible to characterize the two levels between which the resonance is observed, as the symmetric and antisymmetric combinations of classical spin states.

To conclude, we have observed resonant peaks in  $Fe_8$  molecules as a function of the magnetic field perpendicular to the easy axes. Our experiments cover the range of frequencies between 37 GHz and 110 GHz which allowed us to detect coherent spin quantum oscillations for different orientations of spin  $S = 10$ .

E. del B. acknowledges support from the University of Barcelona. J. T., and J. M. H. acknowledge support from the CICYT project No. IN96-0027 and the CIRIT project No. 1996-PIRB-00050. This work was supported in part by NHMFL/IHRP 500/5031, and one of us (EdB) acknowledges some support from the NHMFL Visitors Program during his stay. The NHMFL is supported by a contractual agreement between the State of Florida and the National Science Foundation under contract NSF-DMR-95-27035.

- 
- [1] J.R. Friedman, M.P. Sarachik, J. Tejada and R. Ziolo, Phys. Rev. Lett. **76**, 3830 (1996).
  - [2] J.M. Hernandez, X.X. Zhang, F. Luis, J. Bartolomé, J. Tejada and R. Ziolo, Europhys. Lett. **35**, 301 (1996).
  - [3] L. Thomas, F. Lioni, R. Ballou, D. Gatteschi, R. Sessoli and B. Barbara, Nature **383**, 145 (1996).
  - [4] E.M. Chudnovsky and J. Tejada. 'Macroscopic Quantum Tunneling of the Magnetic Moment' Cambridge University Press (1998).
  - [5] F. Fominaya, J. Villain, P. Gaudit, J. Chaussy and A. Causchi, Phys. Rev. Lett. **79**, 1126 (1997).
  - [6] F. Luis, J. Bartolomé, J.F. Fernandez, J. Tejada, J.M. Hernandez, X.X. Zhang and R. Ziolo. Phys. Rev. **B55**, 11448 (1997).
  - [7] M. Sales et al., Phys. Rev. B (accepted for publication).
  - [8] J. A. A. J. Perenboom, J. S. Brooks, S. Hill, T. Hathaway, and N. S. Dalal, Phys. Rev. B **58**, 330 (1998).
  - [9] D. A. Garanin and E. M. Chudnovsky, Phys. Rev. **B56**.
  - [10] J. F. Fernández, F. Luis, and J. Bartolomé, Phys. Rev.

- Lett. **80**, 5659 (1998).
- [11] J. Villain, F. Hartmann-Boutron, R. Sessoli, and A. Retori, Europhys. Lett. **27**, 159 (1994).
  - [12] W. Wernsdorfer and R. Sessoli. Science **284**, 133 (1999).
  - [13] A. Garg. Europhys. Lett. **22**, 205 (1993).
  - [14] E. del Barco, Europhys. Lett, **47**, 722-728 (1999).
  - [15] D. D. Awschalom et al., Phys. Rev. Lett, **68**, 3092 (1992).
  - [16] K. Wiedghardt, K. Pohl, I. Jibril and G. Huttner. Angew. Chem. Int. Ed. Engl. **23**, 77 (1984).
  - [17] S. Sangregorio, T. Ohm, C. Paulsen, R. Sessoli and D. Gatteschi. Phys. Rev. Lett. **78**, 4645 (1997).
  - [18] A.L. Barra, P. Debrunner, D. Gatteschi, CH.E. Schulz and R. Sessoli. Europhys. Lett. **35**, 133 (1996).
  - [19] X. X. Zhang, J. M. Hernandez, E. del Barco, J. Tejada, A. Roig, E. Molins, K. Wieghardt, J. Appl. Phys. **85** (1999).
  - [20] C. Delfs et al., Inorg. Chem. **32**, 3099 (1993).
  - [21] R. Caciuffo, G. Amoretti, A. Murani, R. Sessoli, A. Caneschi and D. Gatteschi. Phys. Rev. Lett. **81**, 4744 (1998).
  - [22] Manufactured by Abmm, 52 Rue Lhomond, 75005 Paris, France.